Opt Quant Electron
DOI 10.1007/s11082-012-9584-x

Raman response function and Raman fraction of phosphosilicate fibers

Guillermo Salceda-Delgado · Alejandro Martinez-Rios · Boaz Ilan · David Monzon-Hernandez

Received: 22 November 2011 / Accepted: 2 May 2012

Abstract The Raman response function and Raman nonlinear index of phosphosilicate fibers are calculated for several P_2O_5 concentrations. The nonlinear index of phosphosilicate fiber is estimated by using the Boling formula, and it is used to calculate the Raman fraction of the nonlinear index. On the other hand, the Raman response function of the phosphosilicate fibers is fitted to a superposition of six phase-shifted under-damped functions in order to use it in the numerical simulation of ultra-short pulse propagation. We show through numerical simulations that phosphosilicate fibers are a suitable medium to observe a scaling up of the Raman self-frequency shift when compared to silica fibers.

Keywords Raman gain · Raman fraction · Raman response function · Phosphosilicate fiber

1 Introduction

Stimulated Raman scattering (SRS) in optical fibers is a nonlinear effect where part of the energy of a pump wave is transferred to another Stokes wave of lower frequency (Agrawal 2007). In some cases this effect is detrimental for the operation of optical fiber systems (Agrawal 2007), but also can be used to amplify and generate laser light in a wide range of wavelengths (Bertoni 1997; Dianov et al. 1997; Prabhu et al. 2000). The energy transfer rate between pump and Stokes waves depends on several parameters, being the Raman gain characteristics of the material composition the most important, in our case the core composition (Galeener et al. 1978). Two of the core compositions that have received more attention are SiO_2–GeO_2 (Germanium-doped fiber) and SiO_2–P_2O_5(Phosphosilicate-doped fiber), mainly

G. Salceda-Delgado · A. Martinez-Rios (✉) · D. Monzon-Hernandez
Centro de Investigaciones en Óptica, Lomas del Bosque 115, Colonia Lomas del Campestre, 37150 León, Guanajuato, Mexico
e-mail: amr6@cio.mx

B. Ilan
School of Natural Sciences, University of California, Merced, CA 95348, USA

Published online: 15 May 2012

due to the higher Raman gain coefficient and higher Raman frequency shift of the generated Stokes wave, respectively (Dianov 2002). In particular, phosphosilicate optical fibers are a suitable medium to reduce the number of cascades in nested or chained cavity Raman fiber lasers due to their large 1,330 cm^{-1} Raman shift (Dianov et al. 1997; Prabhu et al. 2000; Demidov et al. 2003, Anzueto-Sanchez et al. 2006). In addition, early experimental demonstrations showed that phosphosilicate fibers are also a convenient medium to generate high energy femtosecond pulses (Gouveia-Neto 1992).

On the other hand, in the propagation of ultrashort pulses the description of the Raman effect in terms of a Raman response function is more convenient, due to the fact that the pulse width can be of the order of the Raman shift (Stolen et al. 1989). In other terms, if the spectral width of the pulse exceeds a few terahertz, the high frequency components of the pulse transfer energy to the low frequency components (Agrawal 1990), a effect referred as Raman self-frequency shift which, is best described in terms of the Raman response function The Raman response function describes the delayed temporal response of the nonlinearity, which physically can be thought as arising when two coincident optical fields (the intensity of the high frequency components of the pulse) produce an initial distortion on the molecules and then a third optical field (the lower frequency components of the pulse) arrives to realize the nonlinearity before the memory of the distortion completely fades away (Tang and Sutherland 1997; Martínez-Rios et al. 2001). Analytical forms of the Raman response function have been proposed in order to simplify the numerical calculations (Blow and Wood 1989; Lin and Agrawal 2006; Hollenbeck and Cantrell 2002). Blow and Wood (1989) modeled the Raman response as a single damped oscillation which corresponds to a Raman gain with a Lorentzian profile, while Lin and Agrawal (2006) proposed a function that accounts for the anisotropic part of the Raman response, which was introduced in order to obtain a better fit to the actual Raman gain. On the other hand, Hollenbeck and Cantrell (2002) obtained a more accurate fitting of the Raman response function by the superposition of 13 functions, obtained by assuming an inhomogeneous distribution of damped oscillators. It is worth to mention that the proposed Raman response functions correspond to the case of pure silica fiber, while it is well known that the response function varies with the composition of the core fiber being larger for GeO_2 doped fibers (Rottwith and Povlsen 2005). In this way, it will be useful to calculate the Raman contribution to the nonlinear index and have an analytical Raman response function for phosphosilicate fibers in order to simplify the numerical calculations, particularly for the study of ultrashort pulse propagation.

In this work we calculate the Raman contribution to the nonlinear index in phosphosilicate fibers. In addition, we propose an alternative Raman response function which consists in the superposition of only six under-damped phase shifted functions to fit the Raman response of phosphosilicate fibers. The obtained fitting functions reproduce with good accuracy the Raman gain and Raman nonlinear index spectra. By solving numerically the generalized nonlinear Schrodinger equation we show that phosphosilicate fibers experience a higher self-frequency shift compared to silica fiber under similar conditions.

2 Raman gain of phosphosilicate fibers

In this work we will assume that Raman gain of phosphosilicate fiber can be expressed as the linear superposition of the Raman gain due to SiO_2 and the Raman gain due to P_2O_5, weighted by the molar fraction. However, instead of taking the Raman gain spectrum of pure P_2O_5, we take the Raman gain of P_2O_5 as that extracted from a known phosphosilicate fiber. Since in a real phosphosilicate fiber the Raman gain spectrum has contributions from

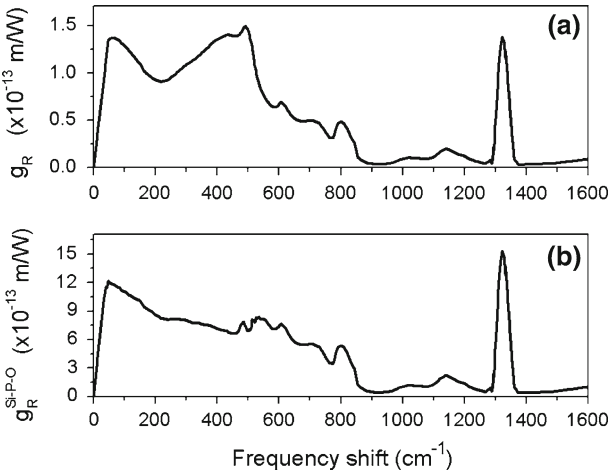

Fig. 1 **a** Raman gain spectrum of a fiber doped with 9 mol% of P_2O_5; **b** calculated Raman gain spectrum of $g_R^{\mathrm{Si-P-O}}$

several vibrational modes arising from O=P double bonds, Si–O–Si, P–O–Si and P–O–P (Plotnichenko et al. 2002), we write the composed Raman gain in a phosphosilicate fiber as,

$$g_R^{\mathrm{SiO_2-P_2O_5}} = X_{\mathrm{SiO_2}} g_R^{\mathrm{SiO_2}} + X_{\mathrm{P_2O_5}} g_R^{\mathrm{Si-P-O}} \tag{1}$$

where X denotes the molar fraction, and $g_R^{\mathrm{SiO_2-P_2O_5}}$ is the Raman gain coefficient of the phosphosilicate fiber. Written in this form, it is assumed that we can separate the sole contribution from silica in a single term $\left(X_{\mathrm{SiO_2}} g_R^{\mathrm{SiO_2}}\right)$, which is an assumption frequently found in literature (Dianov et al. 2000). On the other hand, in the term written as $X_{\mathrm{P_2O_5}} g_R^{\mathrm{Si-P-O}}$, we are assuming that this term contains the part of the Raman spectrum arising from O=P double bonds, P–O–Si and P–O–P linkages. Thus by knowing the Raman gain spectrum of pure silica and a phosphosilicate fiber doped with a given P_2O_5 concentration (9 mol% in Fig. 1a), we can extract a Raman gain spectrum for $g_R^{\mathrm{Si-P-O}}$ (Fig. 1b) and use to estimate the Raman gain spectrum for several concentrations of P_2O_5. It is worth to note that the last assumptions may not be accurate enough to be a valid generalization for all types of phosphosilicate fibers, since the Raman gain characteristics also depend on the fabrication process.

In the calculation of the Raman gain spectrum of phosphosilicate fibers we approximate the peak Raman gain at 1,330 cm^{-1} frequency shift by the following relation, which was obtained from published experimental values at different concentrations and wavelengths (Kazunori et al. 1986; Dianov 2002):

$$g_R^{\mathrm{P_2O_5}} \left(\times 10^{-13} \frac{m}{W}\right) = \frac{0.0735825}{\lambda_{\mathrm{P}}} \left(X_{\mathrm{P_2O_5}} - 0.239584\right) \tag{2}$$

where λ_{P} is the pump wavelength. Figure 2 shows the Raman gain spectrum for P_2O_5 concentrations of 3 mol% (solid curve), 6 mol% (dashed curve), 9 mol% (dotted curve), 11 mol% (dash-dotted curve), 14 mol% (dash-dotted-dotted curve), 17 mol% (short-dashed curve) and 20 mol% (short-dotted curve). All these curves were obtained from Fig. 1 by using relations (1) and (2).

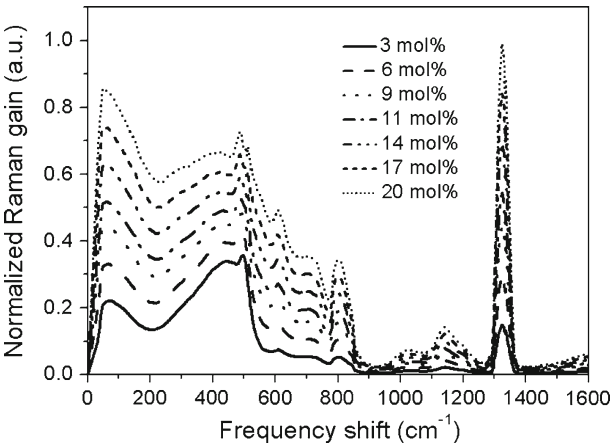

Fig. 2 Normalized Raman gain spectrum for several P_2O_5 concentrations

3 Raman nonlinear index

The changes in the refractive index caused by the Raman effect are associated with the real portion of the Raman susceptibility. Since usually the only data available is the Raman gain spectrum, it is necessary to generate the Raman nonlinear index spectrum from the Raman gain spectrum. In linear optics, the real and imaginary parts of the linear susceptibility are related through the Kramers–Kronig relations. However, it has been shown that the Kramers–Kronig dispersion relations involving dispersive-dissipative effects are also valid for susceptibilities of odd order such as the Raman susceptibility (Bassani and Scandolo 1991). The Kramers–Kronig dispersive relations for the parallel Raman susceptibility χ_{Raman} can be written as

$$\text{Re}\left\{\chi_{\text{Raman}}(\Omega')\right\} = \frac{1}{\pi} P \int_{-\infty}^{+\infty} d\Omega \frac{\text{Im}\left\{\chi_{\text{Raman}}(\Omega')\right\}}{\Omega - \Omega'} \tag{3a}$$

$$\text{Im}\left\{\chi_{\text{Raman}}(\Omega')\right\} = -\frac{1}{\pi} P \int_{-\infty}^{+\infty} d\Omega \frac{\text{Re}\left\{\chi_{\text{Raman}}(\Omega')\right\}}{\Omega - \Omega'} \tag{3b}$$

where Re{} and Im{} stand for the real and imaginary parts of their arguments, P denotes the principal value of the integrals, and Ω ($=\omega_P - \omega_S$) is the frequency difference between the pump and Stokes waves, i.e., the Raman frequency shift.

The integrals in (3) can be considered as the convolution of the Fourier transforms of two functions, i.e.,

$$\begin{aligned}\text{Im}\left\{\chi_{\text{Raman}}(\Omega')\right\} &= -\frac{1}{\pi} P \int_{-\infty}^{+\infty} d\Omega \frac{\text{Re}\left\{\chi_{\text{Raman}}(\Omega')\right\}}{\Omega - \Omega'} \\ &= \frac{1}{\pi} P \left\{\left(\frac{1}{\Omega}\right) * \text{Re}\left\{\chi_{\text{Raman}}(\Omega)\right\}\right\}\end{aligned}$$

Since the inverse Fourier transform of the convolution of two functions is equal to the multiplication of the inverse transforms, we may write

$$\int_{-\infty}^{+\infty} d\Omega' \mathrm{Im}\left\{\chi_{\mathrm{Raman}}(\Omega')\right\} = \frac{1}{\pi} P \left\{ \int_{-\infty}^{+\infty} d\Omega' \left(\frac{\exp(i\Omega' t)}{\Omega'}\right) \times \int_{-\infty}^{+\infty} d\Omega' \mathrm{Re}\left\{\chi_{\mathrm{Raman}}(\Omega)\right\} \exp(i\Omega' t) \right\}$$

where now the discontinuity is only the first integral on the right-side. Thus, for the first integral we have

$$\begin{aligned} P \int_{-\infty}^{+\infty} d\Omega' \left(\frac{\exp(i\Omega' t)}{\Omega'}\right) &= \lim_{\substack{a \to -\infty \\ b \to +\infty}} \int_{a}^{b} d\Omega' \left(\frac{\exp(i\Omega' t)}{\Omega'}\right) \\ &= \lim_{\substack{a \to -\infty \\ b \to +\infty}} \left(\lim_{\varepsilon \to 0} \int_{a}^{p-\varepsilon} d\Omega' \left(\frac{\exp(i\Omega' t)}{\Omega'}\right) \right. \\ &\quad \left. + \lim_{\varepsilon \to 0} \int_{p+\varepsilon}^{b} d\Omega' \left(\frac{\exp(i\Omega' t)}{\Omega'}\right) \right) \end{aligned}$$

and since p is arbitrary, we obtain

$$\begin{aligned} P \int_{-\infty}^{+\infty} d\Omega' \left(\frac{\exp(i\Omega' t)}{\Omega'}\right) &= \lim_{\varepsilon \to 0} \int_{\varepsilon}^{\infty} d\Omega' \left(\frac{\exp(i\Omega' t) - \exp(-i\Omega' t)}{\Omega'}\right) \\ &= \lim_{\varepsilon \to 0} \int_{\varepsilon}^{\infty} d\Omega' \left(\frac{\sin(\Omega' t)}{\Omega'}\right) \\ &= \pi i \end{aligned}$$

By using this result into (3), we obtain

$$\int_{-\infty}^{+\infty} d\Omega' \mathrm{Re}\left\{\chi_{\mathrm{Raman}}(\Omega')\right\} \exp(i\Omega' t) = -i \int_{-\infty}^{+\infty} d\Omega' \mathrm{Im}\left\{\chi_{\mathrm{Raman}}(\Omega')\right\} \exp(i\Omega' t) \qquad (4)$$

Thus, by performing an inverse Fourier transformation on the Raman gain spectrum followed by a Fourier transformation, we can obtain the corresponding spectrum of the Raman nonlinear index. Figure 3 shows the Raman nonlinear spectra corresponding to the Raman gain spectra of Fig. 2, where we have used the method of repeated Fourier transformation, and the following relations (del Coso and Solis 2004):

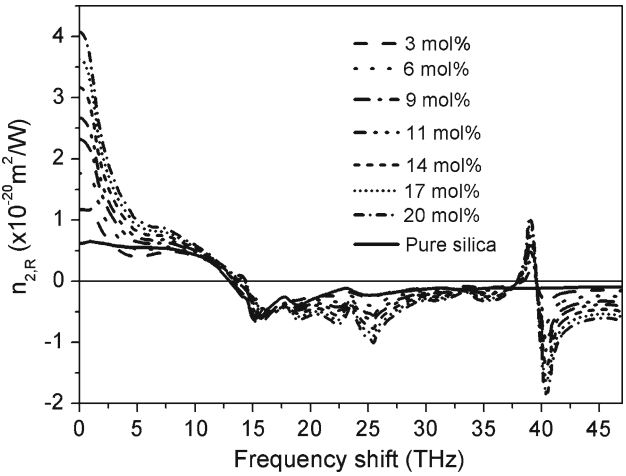

Fig. 3 Spectra of the Raman nonlinear index for several concentration of P_2O_5

$$\mathrm{Re}\left\{\chi_{\mathrm{Raman}}(\Omega')\right\} = \frac{4}{3}n^2\varepsilon_0 c n_{2,R}(\Omega)$$

$$\mathrm{Im}\left\{\chi_{\mathrm{Raman}}(\Omega')\right\} = \frac{n^2\varepsilon_0 c\lambda}{3\pi}g_R(\Omega)$$

where n is the linear refractive index, ε_0 is the permittivity of free space, c is the speed of light, λ is the light wavelength, and $n_{2,\mathrm{R}}$is the Raman nonlinear index.

4 Raman fraction

To obtain the Raman fraction of the nonlinear index used in the definition of the Raman response function we need to know the nonlinear index (electronic plus Raman) of the phosphosilicate fiber. In the case of pure silica, the nonlinear index can be approximated by the following polynomial equation:

$$\begin{aligned} n_2(\lambda) = 1.000055\{&8.30608 - 27.79971\lambda + 59.66014\lambda^2 - 69.24258\lambda^3 \\ &+ 45.22437\lambda^4 - 15.63666\lambda^5 + 2.22585\lambda^6\} \end{aligned} \tag{5}$$

This equation is a polynomial fit of the PERT curve obtained by Milam (1998), who compiled published measured values of the nonlinear index at several wavelengths. Figure 4 shows the nonlinear index of pure silica as a function of wavelength obtained by using relation (5). Here we assume that the nonlinear index in Fig. 4 is the sum of the electronic and Raman contributions at cero frequency shift.

In the case of silica fibers doped with P_2O_5 there are not measured values of the nonlinear index available in literature. Since this value is needed to estimate the Raman fraction, the Boling formula will be used to calculate n_2 in phosphosilicate fibers from known values of refractive index. The Boling formula relates the nonlinear index of a given material with the magnitude and dispersion of the linear refractive index. In particular, the nonlinear index is related to the refractive indices at the Fraunhofer lines d, f and c, and the Abbe number v_d (Boling et al. 1978):

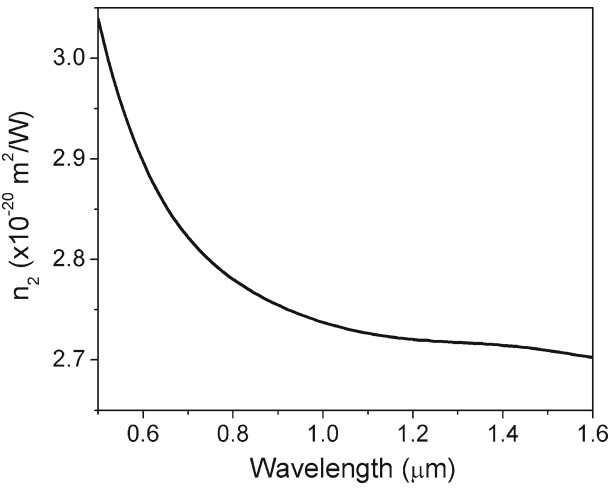

Fig. 4 Nonlinear index of pure silica as a function of wavelength

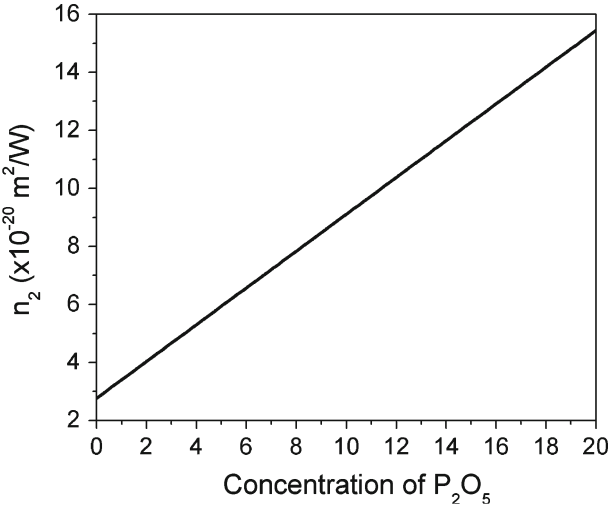

Fig. 5 Nonlinear index of phosphosilicate fiber as a function of P_2O_5 concentration in mol%

$$n_2[\times 10^{-20}\mathrm{m}^2/W] = 2.867 \times \frac{68\,(n_d-1)\left(n_d^2+2\right)^2}{v_d\left[1.52+\frac{(n_d-1)\left(n_d^2+2\right)^2}{6n_d}v_d\right]^{1/2}} \tag{6}$$

where n_f, n_d and n_c are the refractive indices at $\lambda_f = 4.86$ nm, $\lambda_d = 587.6$ nm, $\lambda_c = 656.3$ nm, and

$$v_d = \frac{n_d - 1}{n_f - n_c}$$

Figure 5 shows the nonlinear index of a phosphosilicate fiber as a function of P_2O_5 concentration, where we have used the data for a fiber doped with 9.1 mol% to estimate the value for pure P_2O_5. As in the case of the Raman gain discussed in Sect. 2, the nonlinear index of

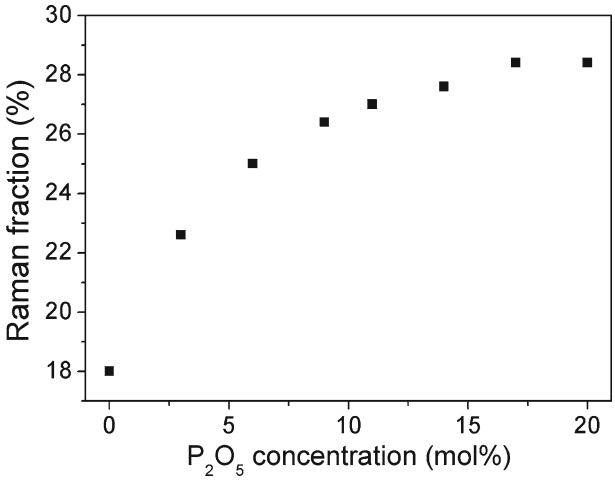

Fig. 6 Raman fraction as a function of P_2O_5 concentration

the phosphosilicate fiber may not be the linear superposition of the nonlinear index due to pure SiO_2 and pure P_2O_5 weighted by the molar fraction of each component. However, in this work it is assumed that the nonlinear index of a phosphosilicate fiber can be expressed as a linear superposition of the following form:

$$n_2^{SiO_2-P_2O_5} = n_2^{SiO_2}\left(1-\chi_{mol\%}\right) + n_2^{P_2O_5}\chi_{mol\%}$$

The Raman fraction is defined as the ratio between the Raman nonlinear index and the total nonlinear index, which here is taken as the value shown in Fig. 5. The Raman fraction as a function of P_2O_5 concentration is shown in Fig. 6.

5 Raman response function

The Raman response function can be obtained from the Raman gain or Raman nonlinear index spectra through a sine or cosine Fourier transform (Stolen et al. 1989). Here, we calculate the Raman response function from the Raman gain spectrum by using the following Fourier transformation (Agrawal 2007),

$$h_R(\tau) = \frac{4n(\omega_P)c}{3\omega_P\chi^{(3)}f_R}\int_{-\infty}^{\infty} g_R(\Omega)e^{-i\Omega\tau}d\Omega \tag{7}$$

which is equivalent to the Fourier sine transform due to the odd character of the Raman gain $g_R(\Omega)$. In addition, $\chi^{(3)}$ is directly related to the nonlinear index by:

$$\chi^{(3)}\left[\frac{m^2}{V^2}\right] = \frac{4\varepsilon_0 cn^2}{3}n_2$$

where n_2 is in m^2/W. Usually, the only known Raman data available for a given material is the Raman gain spectrum. In the case of new materials is more convenient to use (7) to obtain the Raman response function and then, if possible, we can fit the numerically obtained Raman response function to a convenient function, so that, subsequent numerical calculations can be simplified.

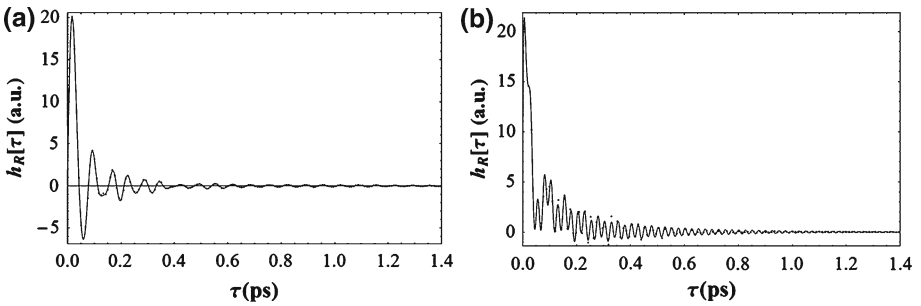

Fig. 7 Raman response function of **a** pure silica fiber, and **b** a phosphosilicate fiber doped with 9.1 mol% P_2O_5. The *dot points* show the values obtained directly from the Raman gain spectrum, and the *solid lines* show the corresponding fitting function

Table 1 Parameters for the fitting functions of silica

i	a_i	b_i	c_i	d_i
1	−1.38286	6.9826	−152.249	0.0235981
2	−2.89047	6.90464	−116.131	0.0662645
3	−23.3933	17.73	−94.064	1.28371
4	−0.68713	2.05146	−93.5428	6.17544
5	1.53569	8.54286	4.81366	2.2266
6	33.1005	59.9305	86.0343	0.701631

Table 2 Parameters for the fitting functions of phosphosilicate fiber

I	a_i	b_i	c_i	d_i
1	−2.42065	3.07206	−252.906	6.32622
2	−2.50814	7.55849	−99.7629	1.6795
3	133.582	74.32972	−72.9659;	2.72893
4	−111.118	94.6436	−0.470369	1.57015
5	65.5615	12.2574	−0.00273249	0.153178
6	50.1704	122.696	180.449	1.60585

In Fig. 7 we plot the Raman response function of pure silica and a phosphosilicate fiber doped with 9.1 mol% of P_2O5, respectively, obtained from Eq.(7). The dotted curve corresponds to the results obtained from the sine transform and the solid line shows the fitting function, which in this case is a superposition of six phase-shifted under-damped functions of the following form:

$$h^R(\tau) = \sum_{i=1}^{n} a_i \exp(-b_i \tau) \sin(c_i \tau + d_i) \tag{8}$$

Increasing the number of functions will result in a higher accuracy, but as can be observed six under-damped fitting functions give an almost perfect match. The coefficients for the fitting function of silica are given in Table 1 and the coefficients for the phosphosilicate fiber are given in Table 2. The fitting expressed by relation (8) is used only to provide a qualitative agreement with the Raman response function obtained directly from the Raman gain

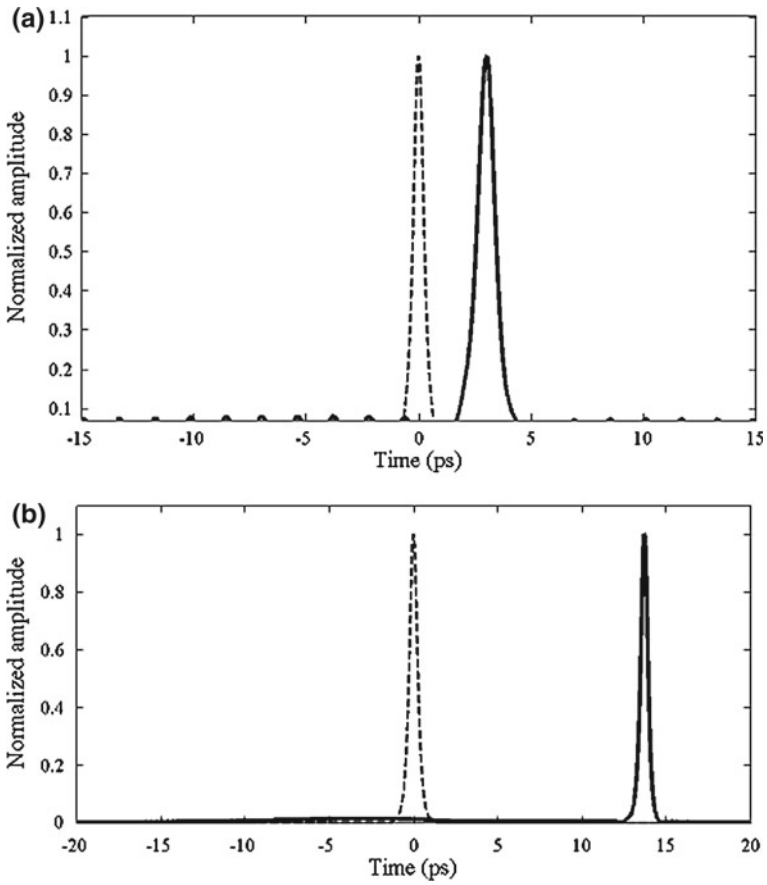

Fig. 8 Pulse profiles for 0.2 ps pump pulses propagated through **a** 500 m of silica fiber (*solid curve*), and **b** 100 m of phosphosilicate fiber (*solid curve*). The *dashed curve* show the input pulse profile

spectrum, and no attempt was made to relate the coefficients to specific Raman resonances. Our future effort will be directed to associate the known central frequencies of Raman resonances (Hollenbeck and Cantrell 2002) with the coefficients c_i of our fitting functions. Since the Fourier transform of Eq.(8) can be evaluated analytically, an analytical expression for the Raman gain in terms of the fitting coefficients may be derived.

6 Raman self-frequency shift

We can observe from the Raman gain spectra of Fig. 2 that the Raman gain of phosphosilicate fiber at frequency shifts as low as ∼1.88 THz is of the order of the peak Raman gains at ∼14.8 and ∼40 THz, which means, for example, that the soliton self-frequency shift is enhanced in a phosphosilicate fiber compared to the case of silica fiber. The objective of this section is to compare the Raman self frequency shift in a pure silica fiber and a phosphosilicate fiber assuming similar input pulse conditions and waveguide parameters. For this purpose we solve the generalized nonlinear Schrodinger equation, given by (Agrawal 2007)

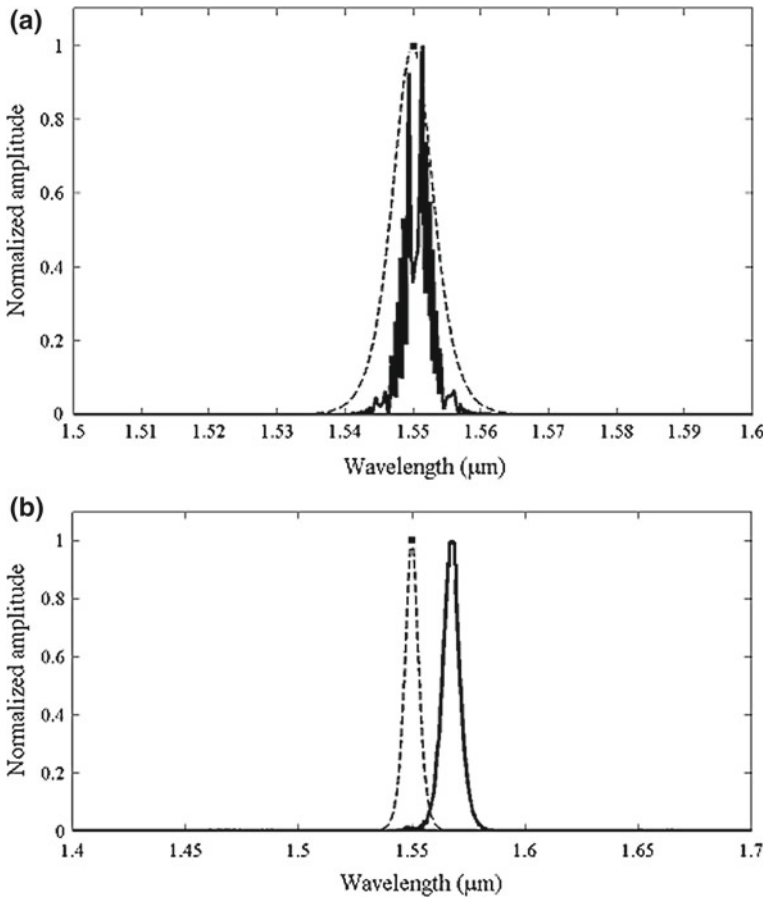

Fig. 9 Output spectrum for 0.2 ps pump pulses propagated through **a** 500 m of silica fiber (*solid curve*), and **b** 100 m of phosphosilicate fiber (*solid curve*). The *dashed curve* show the input pulse spectrum

$$\frac{\partial A(z,t)}{\partial z} + \frac{\beta_2}{2}\frac{\partial^2 A(z,t)}{\partial t^2} = i\gamma\left(1 + \frac{i}{\omega_0}\frac{\partial}{\partial t}\right)\left(A(z,t)\int_0^\infty R(t')\left|A(z,t-t')\right|^2 dt'\right) \quad (9)$$

where $\gamma(= n_2(\omega_0)/(cA_{eff}(\omega_0))$, being ω_0 the central frequency of the pulse, A_{eff} the effective area, and c the spped of light) is the nonlinear coefficient, and A(z,t) is the slowly-varying pulse envelope. In writting Eq. (9) we have neglected losses and the dispersion terms of order higher than 2, i.e., only group velocity dispersion is taken into account.

For the numerical solution of Eq. (9) we consider the following expression:

$$\frac{\partial A(z,t)}{\partial z} = \left(\hat{\mathbf{D}} + \hat{\mathbf{N}}\right) U(z,t) \quad (10)$$

Equation (10) was solved by using the fourth-order Runge-Kutta method in the interaction picture using the following algorithm (Hult 2007):

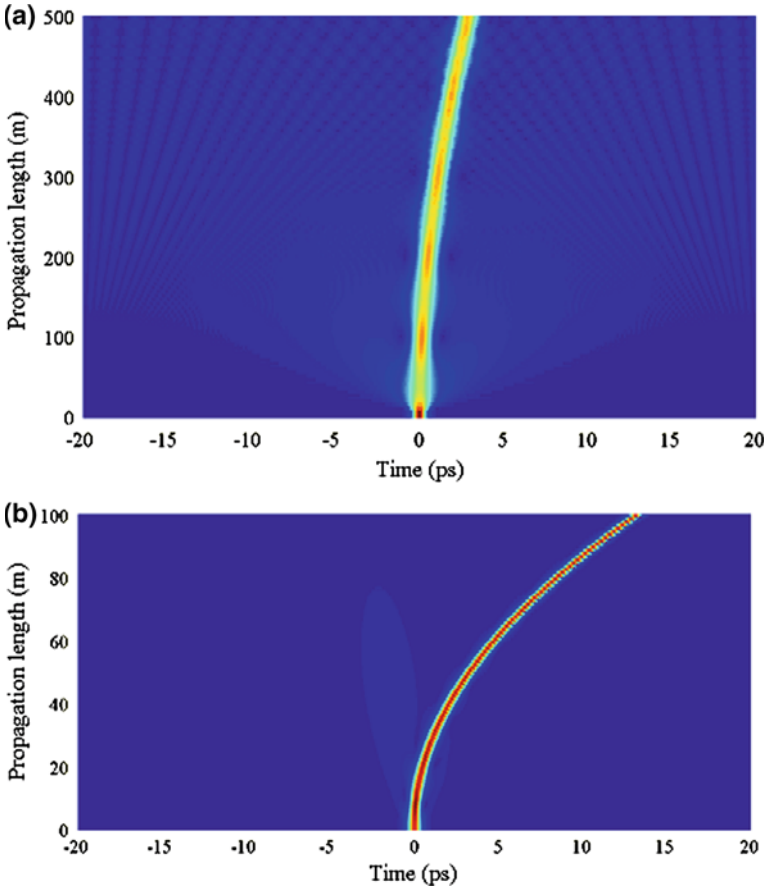

Fig. 10 Density plot of the time evolution of the input pulse with the propagation length for **a** 500 m silica fiber, and **b** 100 m phosphosilicate fiber

$$A_1(z,t) = IFT\left\{\exp\left(\frac{h}{2}\hat{\mathbf{D}}(\omega)\right) FT\left\{A(z,t)\right\}\right\} \tag{11a}$$

$$K_1 = IFT\left\{\exp\left(\frac{h}{2}\hat{\mathbf{D}}(\omega)\right) FT\left\{h\hat{\mathbf{N}}\left(A(z,t)\right)A(z,t)\right\}\right\};$$

$$K_2 = h\hat{\mathbf{N}}\left(A_I(z,t) + K_1/2\right)\left(A_I(z,t) + K_1/2\right) \tag{11b}$$

$$K_3 = h\hat{\mathbf{N}}\left(A_I(z,t) + K_2/2\right)\left(A_I(z,t) + K_2/2\right);$$

$$K_4 = h\hat{\mathbf{N}}\left(IFT\left\{\exp\left(\frac{h}{2}\hat{\mathbf{D}}(\omega)\right) FT\left\{A_I(z,t) + K_3\right\}\right\}\right)$$

$$IFT\left\{\exp\left(\frac{h}{2}\hat{\mathbf{D}}(\omega)\right) FT\left\{A_I(z,t) + K_3\right\}\right\}$$

$$A(z+h,t) = IFT\left\{\exp\left(\frac{h}{2}\hat{\mathbf{D}}(\omega)\right) FT\left\{A_I(z,t) + \frac{K_1}{6} + \frac{K_2}{3} + \frac{K_3}{3}\right\}\right\} + \frac{K_4}{6} \tag{11c}$$

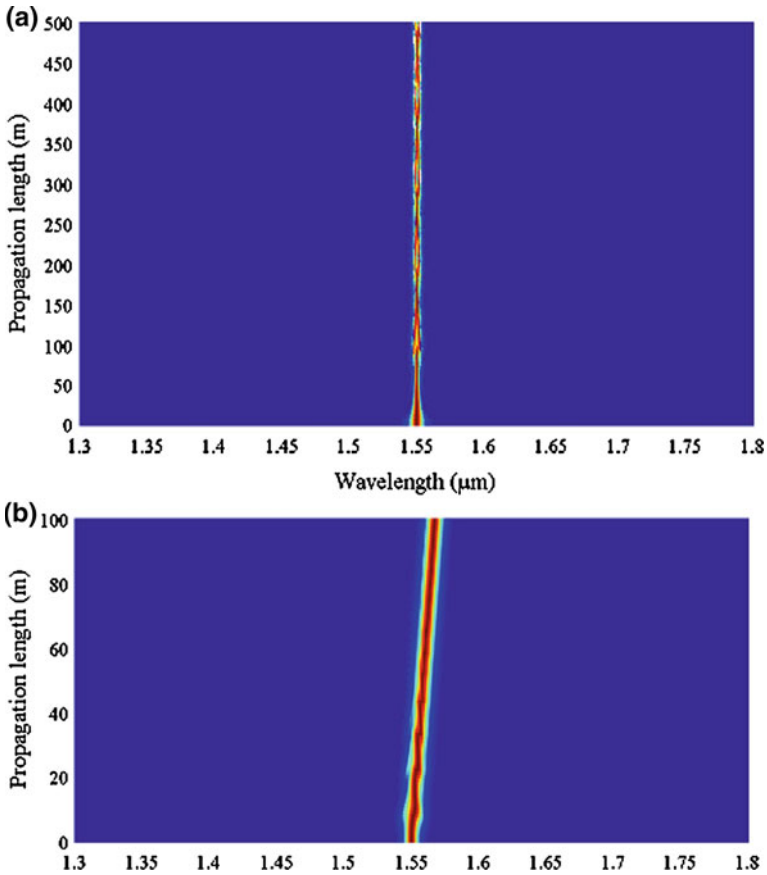

Fig. 11 Density plot of the spectral evolution of the input pulse with the propagation length for **a** 500 m silica fiber, and **b** 100 m phosphosilicate fiber

where the nonlinear operator $\hat{\mathbf{N}}\,(A(z,t))$ is defined as:

$$\begin{aligned}\hat{N}\,(A(z,t)) = \frac{1}{A(z,t)}\Bigg[& i(1-f_R)\left(\gamma\,|A(z,t)|^2\,A(z,t) - 2i\gamma_1\frac{\partial}{\partial t}\left\{A(z,t|^2 A(z,t)\right\}\right) \\ & + i\gamma A(z,t) IFT\left\{\tilde{h}_R(\omega\omega)\,FT\left\{A(z,t)|^2\right\}\right\} \\ & - \gamma_1\frac{\partial}{\partial t}\left\{A(z,t)\,IFT\left\{\tilde{h}_R(\omega\omega)FT\left\{A(z,t)|^2\right\}\right\}\right\}\Bigg] \end{aligned} \tag{12}$$

In relations (10)–(12) FT and IFT denote the Fourier and inverse Fourier's transforms, respectively. In (12) $\tilde{h}_R(\omega)$ is the Fourier transform of the Raman response function defined in this work by Eq.8 and the parameters of Tables 1 and 2, for the case of silica and phosphosilicate fibers, respectively. The input pulse is assumed to be a secant-hyperbolyc with 1.55 μm center wavelength, 0.2 ps pulsewidth, 200 W peak power, and 2^{15} sampling points in the time and frequency domain were used. In addition, the convolution of the Raman response function with the squared absolute value of the field is evaluated in the Fourier domain,

and the time derivative appearing in the nonlinear terms is evaluated by using interpolating functions that are then differentiated.

For the comparison of the Raman self frequency shift in silica and phosphosilicate fiber doped with 9.1 mol% of P_2O_5 we assumed that in both cases the GVD parameter β_2 is -20 ps^2/km. The possible difference in waveguide parameters is not relevant in the comparison since experimentally we may choose a wavelength where the dispersion characteristics are at least of the same order. Solid lines in Figs. 8a and 9a show the time and wavelength shift experienced by the pulse after 500 m propagation through a silica fiber. The maximum Raman shift in this case is $\sim$0.12 THz. In contrast, Figs. 8b and 9b show the time and wavelength shift after propagation through 100 m of phosphosilicate fiber, where the maximum Raman shift is $\sim$2.3 THz. Figures 10 and 11 show density plots of the time and spectral evolution with propagation distance of the input pulse in pure silica and phosphosilicate fibers, respectively. We observe that phosphosilicate fiber scales up the self-frequency shift experienced by the pulse compared to silica, where we would require longer lengths or higher power to obtain a similar effect. This scaling up of the self-frequency shift with the addition of dopants such as GeO_2, with higher Raman gain, was predicted by Mitschke and Mollenauer just after this effect was discovered (Mitschke and Mollenauer 1986). However, GeO_2-doped fibers do not have as high Raman gain as phosphosilicate fibers for small Raman frequency shifts. Hence, phosphosilicate fiber, with a high Raman gain even for small frequency shifts, is a suitable medium to observe this scaling up. This means that the necessary pulse widths and power levels to observe the self-frequency shift and associated effects such as supercontinuum generation are much lower compared to silica.

7 Conclusions

In conclusion we have calculated the Raman nonlinear index in phosphosilicate fiber as a function of P_2O_5 concentration. The Raman fraction was obtained by taking the ratio between the Raman nonlinear index and the total nonlinear index estimated from the Boling formula. In addition we have fitted the Raman gain spectra of silica and phosphosilicate fibers to a superposition of six under-damped phase shifted functions. The fit function of phosphosilicate fiber was used to demonstrate the scaling up of the Raman self-frequency shift compared to the case of silica. Under the same pump conditions and similar waveguide characteristics, the Raman self-frequency shift in 100 m of phosphosilicate fiber was 2.3 THz, while a Raman self-frequency shift of 0.12 THz was obtained in 500 m of silica fiber. In this way, phosphosilicate fibers are advantageous in the study of ultra-short pulse propagation dynamics since the necessary pulse widths and/or power levels to observe soliton self-frequency shift and associated phenomena such as supercontinuum generation, are much lower than in the case of silica fibers.

Acknowledgments Alejandro Martinez Rios wants to acknowledge the financial support provided by University of California Institute for Mexico and the United States (UC MEXUS) and CONACYT México.

References

Agrawal, G.P.: Effect of intrapulse stimulated Raman scattering on soliton-effect pulse compression in optical fibers. Opt. Lett. **15**, 224–226 (1990)

Agrawal, G.P.: Nonlinear Fiber Optics, 4th edn. Academic Press, San Diego (2007)

Anzueto-Sanchez, G., Martinez-Rios, A., Torres-Gomez, I., Selvas-Aguilar, R., Starodumov, A.N.: Characterization of an intra-cavity pumped P_2O_5-doped silica Raman fiber laser. Opt. Rev. **13**, 424–426 (2006)

Bassani, F., Scandolo, S.: Dispersion relations and sum rules in nonlinear optics. Phys. Rev. B. **44**, 8446–8453 (1991)

Bertoni, A.: Analysis of the efficiency of a third order cascaded Raman laser operating at the wavelength of 1.24 μm. Opt. Quantum Electron. **29**, 1047–1058 (1997)

Blow, K.J., Wood, D.: Theoretical description of transient stimulated Raman scattering in optical fibers. IEEE J. Quantum Electron. **25**, 2665–2673 (1989)

Boling, L.N., Glass, J.A., Owyoung, A.: Empirical relationships for predicting nonlinear refractive index changes in optical solids. IEEE J. Quantum Electron. **14**, 601–608 (1978)

Dianov, E.M.: Advances in Raman fibers. J. Lightwave Technol. **20**, 1457–1462 (2002)

Dianov, E.M., Grekov, M.V., Bufetov, I.A., Vasiliev, S.A., Medvedkov, O.I., Plotnichenko, V.G., Koltashev, V.V., Belov, A.V., Bubnov, M.M., Semjonov, S.L., Prokhorov, A.M.: CW high power 1.24 μm and 1.48 μm Raman lasers based on low loss phosphosilicate fiber. Electron. Lett. **33**, 1542–1544 (1997)

Dianov, E.M., Bufetov, I.A., Bubnov, M.M., Grekov, M.V., Vasiliev, S.A., Medvedkov, O.I.: Three-cascaded 1407-nm Raman laser based on phosphorus-doped silica fiber. Opt. Lett. **25**, 402–404 (2000)

del Coso, R., Solis, J.: Relation between nonlinear refractive index and third-order susceptibility in absorbing media. J. Opt. Soc. Am. B. **21**, 640–644 (2004)

Demidov, A.A., Starodumov, A.N., Li, X., Martinez-Rios, A., Po, H.: Three-wavelength Raman fiber laser with reliable dynamic control. Opt. Lett. **28**, 1540–1542 (2003)

Galeener, F.L., Mikkelsen, J.C., Geils, R.H., Mosby, W.J.: The relative Raman cross sections of vitrous SiO_2, GeO_2, B_2O_3, and P_2O_5. Appl. Phys. Lett. **32**, 34–36 (1978)

Gouveia-Neto, A.S.: Modulation instability and soliton-Raman generation in P_2O_5 doped silica fiber. J. Lightwave Technol. **10**, 1536–1539 (1992)

Hollenbeck, D., Cantrell, C.D.: Multiple-vibrational-mode for fiber-optic Raman gain spectrum and response function. J. Opt. Soc. Am. B. **19**, 2886–2892 (2002)

Hult, J.: A fourth-order Runge–Kutta in the interaction picture method for simulating supercontinuum generation in optical fibers. J. Lightwave Technol. **25**, 3770–3775 (2007)

Kazunori, S., Kazuhiro, N., Naoshi, U.: Selective stimulated Raman scattering an highly P_2O_5-doped silica single-mode fibers. Opt. Lett. **11**, 656–658 (1986)

Lin, Q., Agrawal, G.P.: Raman response function for silica fibers. Opt. Lett. **21**, 3086–3088 (2006)

Martínez-Rios, A., Starodumov, A.N., Barmenkov Yu, O., Filippov, V.N., Torres-Gomez, I.: Influence of the symmetry rules for Raman susceptibility on the accuracy of nonlinear index measurements in optical fibers. J. Opt. Soc. Am. B. **18**, 794–803 (2001)

Milam, D.: Review and assesment of measured values of the nonlinear refractive index coefficient of fused silica. Appl. Opt. **37**, 546–550 (1998)

Mitschke, F.M., Mollenauer, L.F.: Discovery of the soliton self-frequency shift. Opt. Lett. **11**, 659–661 (1986)

Plotnichenko, V.G., Sokolov, V.O., Koltashev, V.V., Dianov, E.M.: On the structure of phosphosilicate glasses. J. Non-Cryst. Solids. **306**, 209–226 (2002)

Prabhu, M., Kim, N.S., Ueda, K.: Simultaneous double-color continuous wave Raman fiber laser at 1239 nm and 1484 nm using phosphosilicate fiber. Opt. Rev. **7**, 277–280 (2000)

Rottwith, K., Povlsen, J.H.: Analyzing the fundamental properties of Raman amplification in optical fibers. J. Lightwave Technol. **23**, 3597–3605 (2005)

Stolen, R.H., Gordon, J.P., Tomlinson, W.J., Haus, H.A.: Raman response function of silica-core fibers. Opt. Lett. **6**, 1159–1161 (1989)

Tang, N., Sutherland, R.L.: Time-domain theory of pump-probe experiments with chirped pulses. J. Opt. Soc. Am. B. **14**, 3412–3423 (1997)